

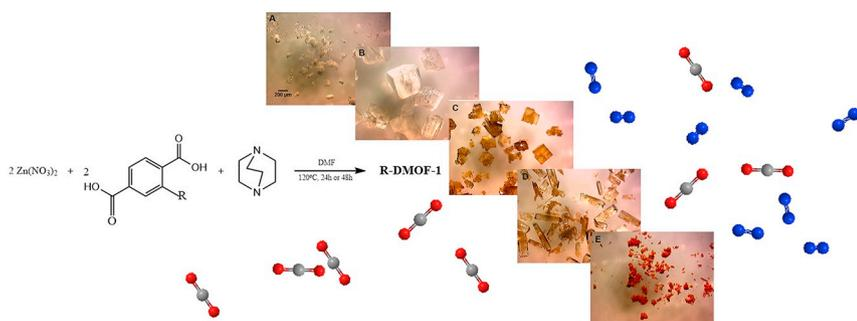


Short communication

## Systematic screening of DMOF-1 with NH<sub>2</sub>, NO<sub>2</sub>, Br and azobenzene functionalities for elucidation of carbon dioxide and nitrogen separation properties

Mingrou Xie<sup>a,1</sup>, Nicholas Prasetya<sup>a,1</sup>, Bradley P. Ladewig<sup>a,b,\*</sup><sup>a</sup> Barrer Centre, Department of Chemical Engineering, Imperial College London, Exhibition Road, London SW7 2AZ, United Kingdom<sup>b</sup> Institute for Micro Process Engineering (IMVT), Karlsruhe Institute of Technology, Hermann-von-Helmholtz-Platz 1, 76344 Eggenstein-Leopoldshafen, Germany

## GRAPHICAL ABSTRACT



## ARTICLE INFO

## Keywords:

Metal organic framework  
DMOF-1  
CO<sub>2</sub> capture and separation

## ABSTRACT

In this study, dabco MOF-1 (DMOF-1) with four different functional groups (NH<sub>2</sub>, NO<sub>2</sub>, Br and azobenzene) has been successfully synthesized through systematic control of the synthesis conditions. The functionalised DMOF-1 is characterized using various analytical techniques including PXRD, TGA and N<sub>2</sub> sorption. The effect of the various functional groups on the performance of the MOFs for post-combustion CO<sub>2</sub> capture is evaluated. DMOF-1s with polar functional groups are found to have better affinity with CO<sub>2</sub> compared with the parent framework as indicated by higher CO<sub>2</sub> heat of adsorption. However, imparting steric hindrance to the framework as in Azo-DMOF-1 enhances CO<sub>2</sub>/N<sub>2</sub> selectivity, potentially as a result of lower N<sub>2</sub> affinity for the framework.

Since its first report in 2004 [1], Dabco MOF-1 (DMOF-1) has been widely investigated, particularly because it has a flexible framework [2,3]. Other investigations have also shown the promising application of this material for gas storage [4–6]. In this study, we then aim to further investigate the applicability of this material for post-combustion CO<sub>2</sub> separation by functionalizing the parent framework with various

functional groups. By changing the synthesis mixture of DMOF-1, various functionalized DMOF-1s could then be successfully synthesized and the molar ratio between the functionalized ligands and the dabco could be maintained at around 2:1 as also found in DMOF-1 as their parent framework (Figs. S2–S6). As can be seen in Fig. 1 both NH<sub>2</sub>-DMOF-1 and Azo-DMOF-1 crystallized in a rod-shape form while the

\* Corresponding author at: Institute for Micro Process Engineering (IMVT), Karlsruhe Institute of Technology, Hermann-von-Helmholtz-Platz 1, 76344 Eggenstein-Leopoldshafen, Germany.

E-mail address: [bradley.ladewig@kit.edu](mailto:bradley.ladewig@kit.edu) (B.P. Ladewig).

<sup>1</sup> Equal contribution.

<https://doi.org/10.1016/j.inoche.2019.107512>

Received 12 July 2019; Received in revised form 6 August 2019; Accepted 7 August 2019

Available online 07 August 2019

1387-7003/ © 2019 Elsevier B.V. All rights reserved.

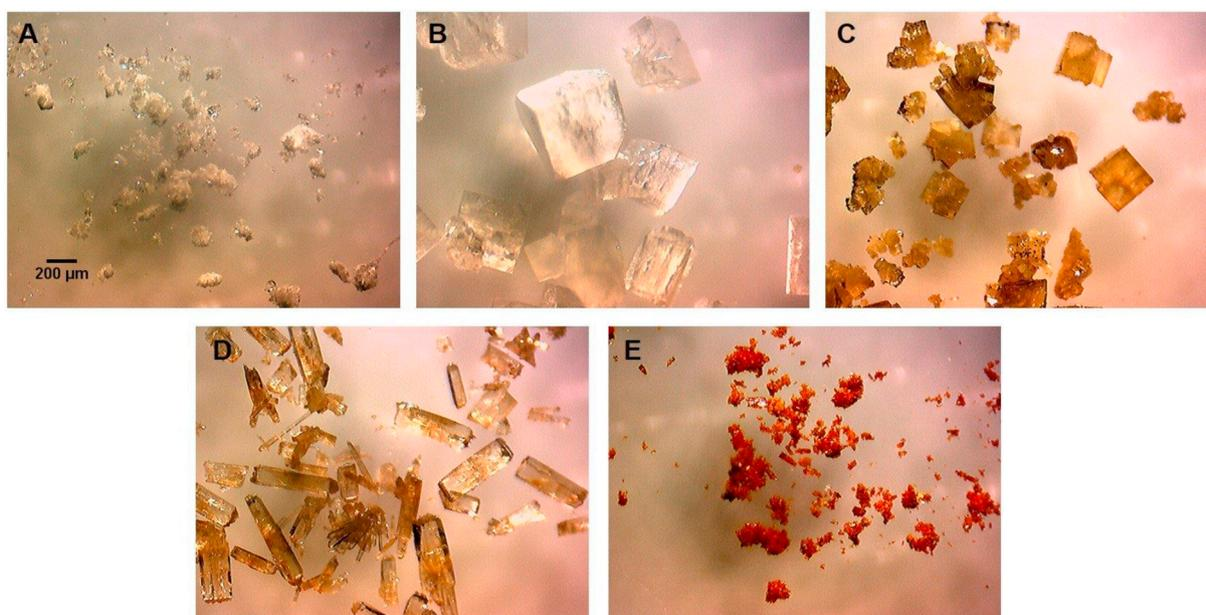


Fig. 1. Microscope image of DMOF-1 (A), Br-DMOF-1 (B), NO<sub>2</sub>-DMOF-1 (C), NH<sub>2</sub>-DMOF-1 (D) and Azo-DMOF-1 (E) synthesized in this study (the scalebar is the same for all panels).

DMOF-1, Br-DMOF-1 and NO<sub>2</sub>-DMOF-1 crystallized in a cubical form.

The product crystallinity was assessed using powder X-ray diffraction (PXRD). As can be seen in Fig. 2(A), all the synthesized materials are highly crystalline with the PXRD diffraction patterns of the functionalized DMOF-1s closely matching that of the non-functionalized DMOF-1, with a few notable differences. Firstly, the intensity of the first two peaks of Br-DMOF-1 are identical, which might be caused by crystals that crystallize in an orthorhombic space group with a rhomboidal pore shape compared with the distorted pore shape from its

parent structure [7,8]. There is also a slight difference observed in the PXRD diffraction pattern of the Azo-DMOF-1 at lower angles where the peak slightly shifts to a lower value. This might be caused by the accommodation process of the bulky structure from the azobenzene ligand [9]. As previously suggested, the presence of the benzene ring from the azobenzene functionality might slightly alter the DMOF-1 parent framework to more closely resemble the PXRD pattern of benzene-loaded DMOF-1 [1].

The thermal stability of the materials was evaluated by heating in

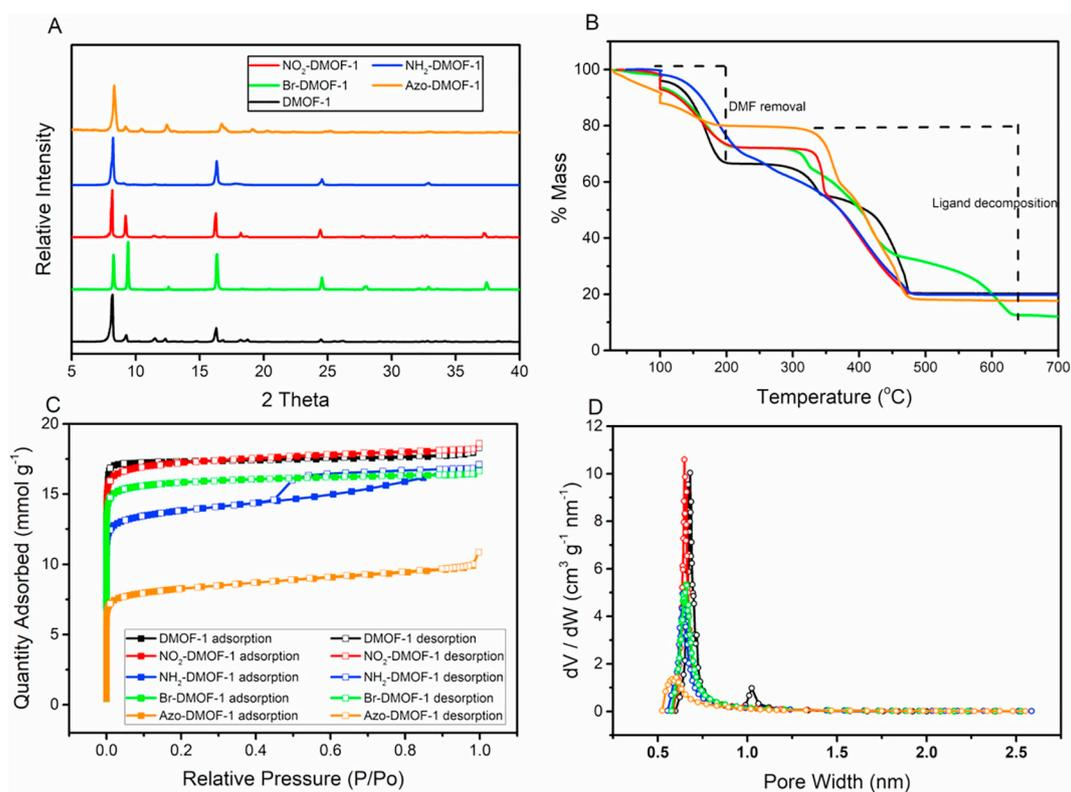


Fig. 2. PXRD diffraction pattern (A), TGA analysis (B), N<sub>2</sub> sorption at 77 K (C) and pore width distribution (D) of functionalized DMOF-1s synthesized in this study.

air in a thermogravimetric analyser, with the combined results presented in Fig. 2(B). Regardless of the DMOF-1 functionalisation, there are three different stages of mass loss. The first region likely results from the removal of DMF from the framework as DMF was the solvent used to synthesize the materials. The second and third step could then be ascribed to the two-step structural decomposition of the framework, since the MOFs were built from two different ligands which may decompose at distinctly different temperatures. However, a different behaviour was found in NH<sub>2</sub>-DMOF-1. It was found that almost no stable region could be observed between 200 and 300 °C as observed with the rest of the MOFs. Rather, the mass was observed to continuously decrease within this range. As will be explained later, this behaviour might be caused by structural imperfection exhibited by the NH<sub>2</sub>-DMOF-1 that might also impact its thermal stability behaviour.

The porosity of all functionalized DMOF-1 was analyzed via N<sub>2</sub> sorption isotherm collected at 77 K, and the results are presented in Fig. 2(C). Almost all the DMOF-1s synthesized in this study exhibit type-1 adsorption isotherms indicating the microporous structure of the functionalized DMOFs. However, a hysteresis does exist for NH<sub>2</sub>-DMOF-1 which suggests the presence of a mesoporous region. This finding then confirms a recent study showing the hysteresis obtained in NH<sub>2</sub>-DMOF-1 which might be caused by the presence of 1D Zn<sub>2</sub>(H<sub>2</sub>O)<sub>2</sub>(NH<sub>2</sub>-BDC) and amorphous NH<sub>2</sub>-DMOF-1 structure during the formation of perfect crystalline NH<sub>2</sub>-DMOF-1 [10]. Their presence then contributes in building linker defects and a more flexible structure in the final DMOF-1 resulting in a mesoporous structure.

Table 1 then presents the BET surface area, maximum pore volume and median pore width of the MOFs used in this study. As can be seen, functionalizing DMOF-1 framework with NO<sub>2</sub> and Br does not then seem to negatively impact its surface property as they have a comparable value with the parent framework. Meanwhile lower surface area and pore volume exhibited by the NH<sub>2</sub>-DMOF-1 compared with both NO<sub>2</sub>-DMOF-1 and Br-DMOF-1 might be explained by the presence of structural imperfection as shown above in the hysteresis explanation in its N<sub>2</sub> sorption. In case of Azo-DMOF-1, the lowest surface area and pore volume is likely be caused by the bulkier structure of azobenzene functionality than for the other functional groups. In contrast, all the functionalized DMOF-1s had lower pore width in the range of 0.63–0.68 nm compared with its parent DMOF-1 which was found around 0.69 nm. The slight reduction of pore width could then be explained by the presence of various protruding functional groups inside the frameworks.

A further evaluation was then carried out to study the performance of various functionalized DMOF-1s for post-combustion CO<sub>2</sub> capture application since the polar functional groups could improve the CO<sub>2</sub> adsorption and separation property in MOFs [11]. This study was then carried out first by measuring the CO<sub>2</sub> uptake capacity of all the MOFs both at 273 and 298 K with the results presented in Fig. 3(A) and (B), respectively. First, as can be seen, the CO<sub>2</sub> uptake of DMOF-1 was found to be around 4.2 and 1.6 mmol g<sup>-1</sup> at 273 and 298 K. These values are also comparable with other findings reported on DMOF-1 [12]. Once functionalized ligands were used in DMOF-1, varieties were observed regarding this value. The CO<sub>2</sub> adsorption capacity in Br-DMOF-1 was observed to be around 4.6 and 1.9 mmol g<sup>-1</sup> at 273 and 298 K, respectively. Meanwhile an increasing trend could be observed both in

NH<sub>2</sub>-DMOF-1 and NO<sub>2</sub>-DMOF-1. In NH<sub>2</sub>-DMOF-1, this value could be increased to be around 5.5 and 2.5 mmol g<sup>-1</sup> at 273 and 298 K, respectively. Meanwhile for NO<sub>2</sub>-DMOF-1, the CO<sub>2</sub> adsorption capacity was found to be around 5.8 and 2.5 mmol g<sup>-1</sup> at 273 and 298 K, respectively. In contrast, a decreasing trend could be observed in Azo-DMOF-1 as its CO<sub>2</sub> uptake capacity was found to be around 2.8 and 1.4 mmol g<sup>-1</sup> at 273 and 298 K, respectively.

From these results, it could be observed that although both NH<sub>2</sub>-DMOF-1 and NO<sub>2</sub>-DMOF-1 have lower surface area compared with the DMOF-1, both amino and nitro group could be considered as polar groups that could enhance the interaction between the MOF framework and CO<sub>2</sub> resulting in overall increase in CO<sub>2</sub> uptake [11,13]. This is also corroborated by the CO<sub>2</sub> heat of adsorption of both MOFs which are found to be around 23 and 25 kJ mol<sup>-1</sup> for NO<sub>2</sub>-DMOF-1 and NH<sub>2</sub>-DMOF-1, respectively, as can be seen in the inset of Fig. 3(B). These values are higher compared with the parent MOF which was found to be around 20 kJ mol<sup>-1</sup> which is comparable with other findings [5,14,15]. The higher CO<sub>2</sub> heat of adsorption value exhibited by both NO<sub>2</sub>-DMOF-1 and NH<sub>2</sub>-DMOF-1 then indicates more favourable interaction between CO<sub>2</sub> and both frameworks rather than DMOF-1. Meanwhile a decreasing trend in CO<sub>2</sub> uptake in Azo-DMOF-1 is expected since it has the lowest surface area compared with the rest of the MOFs used in this study. This then results in the overall reduction of CO<sub>2</sub> uptake capacity of Azo-DMOF-1. Interestingly, the decreasing trend of CO<sub>2</sub> uptake in Azo-DMOF-1 was not accompanied by the decrease of CO<sub>2</sub> heat of adsorption which was found to be around 28 kJ mol<sup>-1</sup> at high coverage. This value is even higher than both NH<sub>2</sub>-DMOF-1 and NO<sub>2</sub>-DMOF-1 and comparable with other MOFs designed for CO<sub>2</sub> capture [16–19]. This then indicates a more favourable interaction between CO<sub>2</sub> and the framework which could be caused by the Lewis acid-base interaction between the CO<sub>2</sub> and azobenzene functionality [20].

Ideal Adsorbed Solution Theory (IAST) was then employed to further evaluate the CO<sub>2</sub>/N<sub>2</sub> separation performance [21]. A scenario of 15:85 mixture of CO<sub>2</sub>:N<sub>2</sub> was used for the calculation in order to simulate the flue gas composition from a coal-fired power plant [22]. The result is then presented in Fig. 3(D). First, it could be seen that the CO<sub>2</sub>/N<sub>2</sub> selectivity of DMOF-1 was found to be around 15 with a total uptake to be around 0.28 mmol g<sup>-1</sup>. This value is also comparable with previous findings when studying DMOF-1 for CO<sub>2</sub>/N<sub>2</sub> separation [14,15]. For the functionalized DMOF-1s, it could be seen that their uptake capacity could be increased compared with the parent MOF. This might be explained by the higher CO<sub>2</sub> uptake capacity and heat of adsorption of the functionalized DMOF-1 which could increase both the capacity and affinity between the functionalized DMOF-1 and the CO<sub>2</sub>. However, only NH<sub>2</sub>-DMOF-1 and Azo-DMOF-1 showed a higher CO<sub>2</sub>/N<sub>2</sub> selectivity value compared with DMOF-1 while a slight decrease was observed both for NO<sub>2</sub>-DMOF-1 and Br-DMOF-1. The CO<sub>2</sub>/N<sub>2</sub> selectivity for Azo-DMOF-1 and NH<sub>2</sub>-DMOF-1 was found to be around 40 and 25, respectively. This selectivity value is comparable, or higher in case of Azo-DMOF-1, with other MOF designed for post-combustion CO<sub>2</sub> capture such as PCN-88 [23], Ni-AG15 [24] and Ni-MOF-1 [25].

This phenomenon could then be explained two ways. First, higher CO<sub>2</sub> heat of adsorption observed in functionalized DMOF-1 might help to increase its affinity with CO<sub>2</sub> resulting in higher selectivity. However, this could not fully explain the phenomenon as higher selectivity was not observed in all functionalized DMOF-1s and the Azo-DMOF-1 had higher selectivity compared with the NH<sub>2</sub>-DMOF-1. Therefore, another mechanism might play a role which is more related with N<sub>2</sub> interaction with the framework. It could be seen in Fig. 3(C) that all the N<sub>2</sub> uptake curves in Azo-DMOF-1 were different to the rest of the functionalized DMOF-1s. The trend was observed to be plateauing rather than linearly increasing as observed with the rest. This might then indicate that the affinity of N<sub>2</sub> with Azo-DMOF-1 is weaker than with the NH<sub>2</sub>-DMOF-1. A decrease in N<sub>2</sub> affinity towards porous framework have also been reported previously in organic-based porous materials [26]. With

**Table 1**  
Surface properties of functionalized DMOF-1s.

| MOF                     | BET surface area (m <sup>2</sup> g <sup>-1</sup> ) | Max pore volume (cm <sup>3</sup> g <sup>-1</sup> ) | Median pore width (nm) |
|-------------------------|--|--|------------------------|
| DMOF-1                  | 1161   | 0.601  | 0.68                   |
| NO <sub>2</sub> -DMOF-1 | 1175   | 0.596  | 0.66                   |
| NH <sub>2</sub> -DMOF-1 | 961.3  | 0.478  | 0.65                   |
| Br-DMOF-1               | 1074   | 0.548  | 0.66                   |
| Azo-DMOF-1              | 579.8  | 0.285  | 0.64                   |

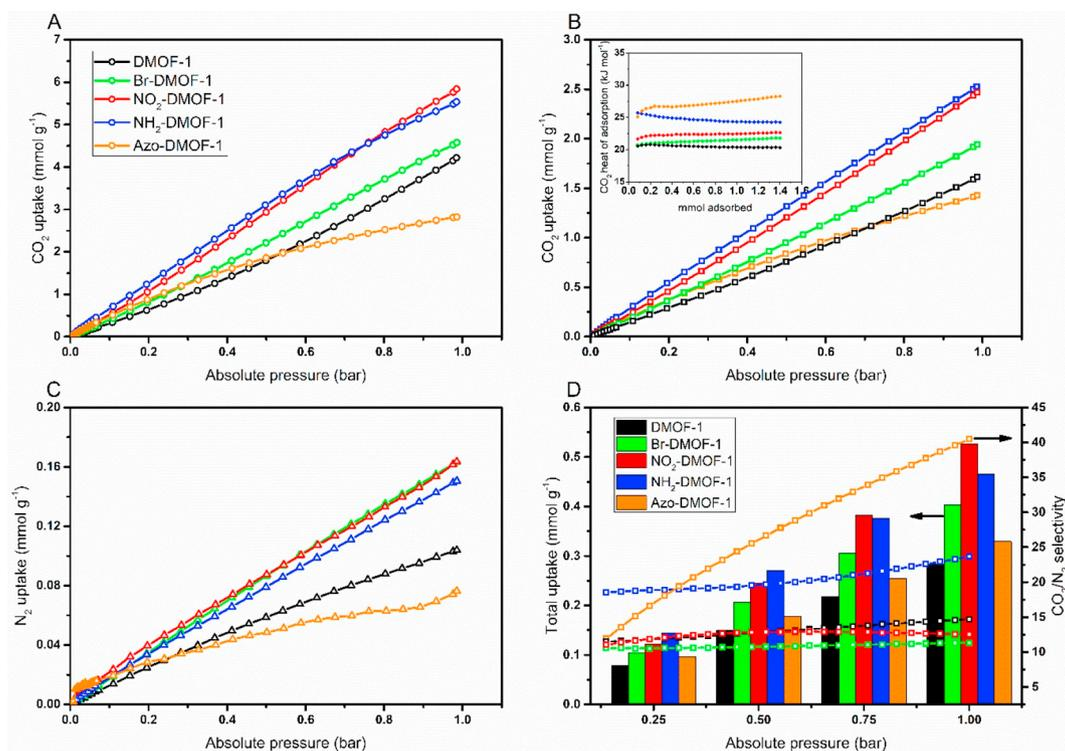


Fig. 3. CO<sub>2</sub> adsorption at 273 K (A) and 298 K (B), N<sub>2</sub> uptake at 298 K (C) and CO<sub>2</sub>/N<sub>2</sub> (15:85) IAST selectivity at 298 K (D) of the functionalized DMOF-1s. Inset of Fig. 3(B): CO<sub>2</sub> heat of adsorption of functionalized DMOF-1s.

higher N<sub>2</sub> concentration than CO<sub>2</sub> in the feed composition, this also means that the competitive adsorption in Azo-DMOF-1 might be less demanding than in the NH<sub>2</sub>-DMOF-1 since the framework of the former is more N<sub>2</sub>-phobic compared with the latter. As a result, the CO<sub>2</sub> would have higher tendency to adsorb on the surface of Azo-DMOF-1 and thus higher selectivity was obtained. This phenomenon was also previously observed with azobenzene-based porous materials where higher CO<sub>2</sub>/N<sub>2</sub> was observed because of the lower affinity between the framework and N<sub>2</sub> [26]. This then highlights the benefit of having azobenzene functionality in DMOF-1 apart from the potential to use UV light as a sustainable source for material regeneration after the CO<sub>2</sub> capture [9,27].

In conclusion, this study has shown that functionalizing DMOF-1s with various functional groups within its framework is beneficial to increase their affinity towards CO<sub>2</sub> as indicated by higher CO<sub>2</sub> heat of adsorption and resulting in higher CO<sub>2</sub> uptake capacity. However, in case where competitive adsorption occurs between CO<sub>2</sub> and N<sub>2</sub>, functionalizing the DMOF-1 with azobenzene group seems to have the best impact since the steric effect of the azobenzene could also impart an additional N<sub>2</sub>-phobic environment in the framework resulting in higher CO<sub>2</sub>/N<sub>2</sub> selectivity. However, in case where CO<sub>2</sub> concentration is higher and less adsorption competition occurs, this steric effect might not be so beneficial since it also hinders the CO<sub>2</sub> adsorption on the surface resulting in slightly lower selectivity and lower CO<sub>2</sub> uptake capacity.

#### Data repository

Full resolution optical and SEM images and high-resolution copies of the figures used in this manuscript are available from the open repository: <https://doi.org/10.5281/zenodo.3332915>.

#### Acknowledgments

N.P. acknowledges the PhD scholarship funding from the Department of Chemical Engineering, Imperial College London. M. X

acknowledges the UROP funding from Department of Chemical Engineering, Imperial College London.

#### Appendix A. Supplementary material

Supplementary data to this article can be found online at <https://doi.org/10.1016/j.inoche.2019.107512>.

#### References

- [1] D.N. Dybtsev, H. Chun, K. Kim, Rigid and flexible: a highly porous metal-organic framework with unusual guest-dependent dynamic behavior, *Angew. Chemie - Int. Ed.* 43 (2004) 5033–5036, <https://doi.org/10.1002/anie.200460712>.
- [2] S. Henke, A. Schneemann, A. Wütscher, R.A. Fischer, Directing the breathing behavior of pillared-layered metal-organic frameworks via a systematic library of functionalized linkers bearing flexible substituents, *J. Am. Chem. Soc.* 134 (2012) 9464–9474, <https://doi.org/10.1021/ja302991b>.
- [3] S. Henke, R. Schmid, J.-D. Grunwaldt, R.A. Fischer, Flexibility and sorption selectivity in rigid metal-organic frameworks: the impact of ether-functionalised linkers, *Chem. - A Eur. J.* 16 (2010) 14296–14306, <https://doi.org/10.1002/chem.201002341>.
- [4] Z. Wang, K.K. Tanabe, S.M. Cohen, Tuning hydrogen sorption properties of metal-organic frameworks by postsynthetic covalent modification, *Chem. - A Eur. J.* 16 (2010) 212–217, <https://doi.org/10.1002/chem.200902158>.
- [5] S. Chaemchuen, K. Zhou, N.A. Kabir, Y. Chen, X. Ke, G. Van Tendeloo, F. Verpoort, Tuning metal sites of DABCO MOF for gas purification at ambient conditions, *Microporous Mesoporous Mater.* 201 (2015) 277–285, <https://doi.org/10.1016/j.micromeso.2014.09.038>.
- [6] H. Kim, D.G. Samsonenko, S. Das, G.-H. Kim, H.-S. Lee, D.N. Dybtsev, E.A. Berdonosova, K. Kim, Methane sorption and structural characterization of the sorption sites in Zn 2 (bdc) 2 (dabco) by single crystal X-ray crystallography, *Chem. - An Asian J.* 4 (2009) 886–891, <https://doi.org/10.1002/asia.200900020>.
- [7] L.K. Cadman, J.K. Bristow, N.E. Stubbs, D. Tiana, M.F. Mahon, A. Walsh, A.D. Burrows, Compositional control of pore geometry in multivariate metal-organic frameworks: an experimental and computational study, *Dalt. Trans.* 45 (2016) 4316–4326, <https://doi.org/10.1039/C5DT04045K>.
- [8] K. Uemura, Y. Yamasaki, F. Onishi, H. Kita, M. Ebihara, Two-step adsorption on jungle-gym-type porous coordination polymers: dependence on hydrogen-bonding capability of adsorbates, ligand-substituent effect, and temperature, *Inorg. Chem.* 49 (2010) 10133–10143, <https://doi.org/10.1021/ic101517t>.
- [9] N. Prasetya, B.P. Ladewig, New azo-DMOF-1 MOF as a photosensitive low-energy CO<sub>2</sub> adsorbent and its exceptional CO<sub>2</sub>/N<sub>2</sub> separation performance in mixed matrix membranes, *ACS Appl. Mater. Interfaces* 10 (2018) 34291–34301, <https://doi.org/10.1021/acsami.8b11111>.

- [doi.org/10.1021/acsami.8b12261](https://doi.org/10.1021/acsami.8b12261).
- [10] D.T. McGrath, V.A. Downing, M.J. Katz, Investigating the Crystal Engineering of the Pillared Paddlewheel Metal-organic Framework  $Zn_2(NH_2BDC)2DABCO^+$ , (2018), <https://doi.org/10.1039/c8ce00848e>.
- [11] G.E. Cmarik, M. Kim, S.M. Cohen, K.S. Walton, Tuning the adsorption properties of UiO-66 via ligand functionalization, *Langmuir* 28 (2012) 15606–15613, <https://doi.org/10.1021/la3035352>.
- [12] Y. Zhao, H. Wu, T.J. Emge, Q. Gong, N. Nijem, Y.J. Chabal, L. Kong, D.C. Langreth, H. Liu, H. Zeng, J. Li, Enhancing gas adsorption and separation capacity through ligand functionalization of microporous metal-organic framework structures, *Chem. - A Eur. J.* 17 (2011) 5101–5109, <https://doi.org/10.1002/chem.201002818>.
- [13] S. Biswas, P. Van Der Voort, A general strategy for the synthesis of functionalised UiO-66 frameworks: characterisation, stability and CO<sub>2</sub> adsorption properties, *Eur. J. Inorg. Chem.* (2013) 2154–2160, <https://doi.org/10.1002/ejic.201201228>.
- [14] Z. Liang, M. Marshall, A.L. Chaffee, CO<sub>2</sub> adsorption, selectivity and water tolerance of pillared-layer metal organic frameworks, *Microporous Mesoporous Mater.* 132 (2010) 305–310, <https://doi.org/10.1016/j.micromeso.2009.11.026>.
- [15] P. Mishra, S. Edubilli, B. Mandal, S. Gumma, Adsorption of CO<sub>2</sub>, CO, CH<sub>4</sub> and N<sub>2</sub> on DABCO based metal organic frameworks, *Microporous Mesoporous Mater.* 169 (2013) 75–80, <https://doi.org/10.1016/j.micromeso.2012.10.025>.
- [16] C. Lv, W. Li, Y. Zhou, J. Li, Z. Lin, A new porous ca(II)-organic framework with acylamide decorated pores for highly efficient CO<sub>2</sub> capture, *Inorg. Chem. Commun.* 99 (2019) 40–43, <https://doi.org/10.1016/j.inoche.2018.11.008>.
- [17] C.-L. Gao, J.-Y. Nie, Preferential CO<sub>2</sub> adsorption and theoretical simulation of a cu (II)-based metal-organic framework with open-metal sites and basic groups, *Inorg. Chem. Commun.* 102 (2019) 199–202, <https://doi.org/10.1016/J.INOCHE.2019.02.029>.
- [18] M.-Y. Sun, D.-M. Chen, A microporous metal-organic framework with unusual 2D → 3D polycatenation for selective sorption of CO<sub>2</sub> over CH<sub>4</sub> at room temperature, *Inorg. Chem. Commun.* 89 (2018) 18–21, <https://doi.org/10.1016/J.INOCHE.2018.01.011>.
- [19] S. Xiang, Y. He, Z. Zhang, H. Wu, W. Zhou, R. Krishna, B. Chen, Microporous metal-organic framework with potential for carbon dioxide capture at ambient conditions, *Nat. Commun.* 3 (2012) 954, <https://doi.org/10.1038/ncomms1956>.
- [20] P. Arab, E. Parrish, T. İslamoğlu, H.M. El-Kaderi, Synthesis and evaluation of porous azo-linked polymers for carbon dioxide capture and separation, *J. Mater. Chem. A* 3 (2015) 20586–20594, <https://doi.org/10.1039/C5TA04308E>.
- [21] S. Lee, J.H. Lee, J. Kim, User-friendly graphical user interface software for ideal adsorbed solution theory calculations, *Korean J. Chem. Eng.* 35 (2018) 214–221, <https://doi.org/10.1007/s11814-017-0269-9>.
- [22] M. Oschatz, M. Antonietti, A search for selectivity to enable CO<sub>2</sub> capture with porous adsorbents, *Energy Environ. Sci.* 11 (2018) 57–70, <https://doi.org/10.1039/C7EE02110K>.
- [23] J.-R. Li, J. Yu, W. Lu, L.-B. Sun, J. Sculley, P.B. Balbuena, H.-C. Zhou, Porous materials with pre-designed single-molecule traps for CO<sub>2</sub> selective adsorption, *Nat. Commun.* 4 (2013) 1538, <https://doi.org/10.1038/ncomms2552>.
- [24] L. Asgharnejad, A. Abbasi, A. Shakeri, Ni-based metal-organic framework/GO nanocomposites as selective adsorbent for CO<sub>2</sub> over N<sub>2</sub>, *Microporous Mesoporous Mater.* 262 (2018) 227–234, <https://doi.org/10.1016/J.MICROMESO.2017.11.038>.
- [25] L. Wang, R. Zou, W. Guo, S. Gao, W. Meng, J. Yang, X. Chen, R. Zou, A new microporous metal-organic framework with a novel trinuclear nickel cluster for selective CO<sub>2</sub> adsorption, *Inorg. Chem. Commun.* 104 (2019) 78–82, <https://doi.org/10.1016/J.INOCHE.2019.03.029>.
- [26] H.A. Patel, S. Hyun Je, J. Park, D.P. Chen, Y. Jung, C.T. Yavuz, A. Coskun, Unprecedented high-temperature CO<sub>2</sub> selectivity in N<sub>2</sub>-phobic nanoporous covalent organic polymers, *Nat. Commun.* 4 (2013) 1357, <https://doi.org/10.1038/ncomms2359>.
- [27] R. Lyndon, K. Konstas, B.P. Ladewig, P.D. Southon, P.C.J. Kepert, M.R. Hill, Dynamic photo-switching in metal-organic frameworks as a route to low-energy carbon dioxide capture and release, *Angew. Chemie Int. Ed.* 52 (2013) 3695–3698, <https://doi.org/10.1002/anie.201206359>.